KSCE Journal of Civil Engineering (2017) 21(4):1386-1392
DOI 10.1007/s12205-016-0983-6

Structural Engineering
pISSN 1226-7988, eISSN 1976-3808
www.springer.com/12205

Uncertainty and Dependence Analysis of Performance Limit State for Structural Multidimensional Fragility Evaluation

Qi'ang Wang*, Ziyan Wu, and Lu Liu*****

Received November 23, 2015/Accepted May 11, 2016/Published Online July 11, 2016

Abstract

Considering uncertainty and dependence of performance limit states (PLSs), the study addresses a methodology to evaluate multidimensional fragility. The purpose is to identify the PLS uncertainty quantitatively. The dependence between each PLS parameters is also investigated. The limit state band is firstly proposed to describe the bi-dimensional case. Through interval estimation, the band area with a certain confidence level is determined. A reinforcement concrete bridge is used as example to illustrate the proposed approach for developing fragility curves. PLS threshold samples are obtained to formulate limit state function using incremental dynamic analysis. The study investigates the sensitivity of the method for fragility assessment when different confidence levels are considered. In addition, influence of correlation coefficient between PLSs is evaluated. Results show that a fragility interval is obtained with the introduction of limit state band. The interval length decreases as with the reduction of the confidence level. The probability of failure becomes smaller when the dependence between PLSs is ignored, which will result in overestimation of the structural seismic performance.

Keywords: *multidimensional fragility, uncertainty, dependence, limit state band, incremental dynamic analysis*

1. Introduction

Uncertainty and dependence are inherent during structural fragility estimation. General, fragility assessment involve uncertainties associated with ground motion, analytical model, experimental measurement errors and epistemic uncertainty (Colangelo, 2013a). There also exist statistical dependences between different seismic responses and performance limit states for structural components. Thus, It is crucial to obtain the fragility prediction with an acceptable degree of credibility considering different kinds of uncertainties and dependences.

The deterministic analysis methods are thought to be insufficient to deal with those problems. Probabilistic analysis approach is introduced into the seismic fragility evaluation, which makes the fragility analyses more accurate and more dependable. Multiple effort were developed for accurate fragility assessment considering different kinds of uncertanties. Karim and Yamazaki (Karim and Yamazaki, 2001) considered randomness of ground motion to construct the empirical fragility curves for highway bridges. Uncertainties of capacity and demand are simultaneously estimated using the ratios of demands to capacities at different limit states (Pan *et al.*, 2007). The influence of finite element model uncertainties is investigated to obtain accurate fragility curves (Pang *et al.*, 2014; Tubaldi *et al*., 2012). Fuzzy algorithm is also proposed to solve the uncertainties and dependences (Colangelo, 2012) in the fragility assessment for a masonry structure. In generally, Researches are challenged with considering various uncertainties while balancing the simulation and computational effort. Few have investigated the influence of Performance Limit State (PLS) uncertainty and dependence simultaneously for structural fragility evaluation. However, PLSs for different components shall be modeled as random and dependent parameters for the actual engineering structure.

This study presents an investigation of the seismic performance limit state uncertainty and dependence for engineering structures. The limit state band is firstly proposed to describe the bi-dimensional PLS uncertainty. Through interval estimation, the bi-dimensional limit state band is determined quantitatively with a confidence level. The correlation coefficient between performance limit states is calculated through nonlinear regression fitting to evaluate PLS dependence. Consequently, fragility curves with a confidence level can be developed. A structural health monitoring

*Assistant Professor, State Key Laboratory for Geomechanics and Deep Underground Engineering, Xuzhou 221116, Jiangsu, China; Assistant Professor, China University of Mining and Technology, School of Mechanics and Civil Engineering, Xuzhou 221116, Jiangsu, China (Corresponding Author, E-mail: qawang@mail.nwpu.edu.cn)
**Professor, School of Mechanics, Civil Engineering and Architecture, Northwestern Polytechnical University, Xi'an 710129, China (E-mail: zywu@mail.nwpu.edu.cn)
***Master, School of Mechanics, Civil Engineering and Architecture, Northwestern Polytechnical University, Xi'an 710129, China (E-mail: liulu91@mail.nwpu.edu.cn)

test structure in UC Irvine is used to illustrate the proposed approach.

2. Methodology

2.1 Multidimensional Fragility

The structural fragility is defined as the probability that structural demand exceeds the structural capacity associated with a damage limit state (Nazri and Saruddin, 2015). The limit states can be defined as internal forces, story drift ratio and acceleration, etc. The traditional fragility definition can be extended to multidimensional fragility (Casciati *et al.*, 2008; Cimellaro *et al.*, 2006):

$$P_f = P\{R_1 \geq r_{\lim 1} \cup R_1 \geq r_{\lim 2} \ldots \cup R_n \geq r_{\lim n} | IM\} \quad (1)$$

R_n is the Engineering Demand Parameter (EDP). $r_{\lim i}$ is the seismic response threshold correlated with different damage level. *IM* is earthquake intensity measurement. The union indicates the aggregation of the conditional probabilities for multiple seismic demand parameters with multiple limit thresholds.

2.2 Multidimensional PLS function

Fragility curves are functions that represent the conditional probability that a structural response to various seismic excitations exceeds a given PLS. It is critical to construct the function of the PLS to find under what condition the structure will be in damage state. Generally, PLS are defined from consensus of engineering and functionality criteria. PLSs for different components shall be regarded as related rather than independent, and they are also should be considered to be random. Thus, a generalized function for multidimensional PLS is constructed as shown in Eq. (2). The generalized multidimensional PLS function provides a tool that allows considering these dependences between different component limit thresholds (Cimellaro and Reinhorn, 2010).

$$L(R_1, R_2, \ldots, R_n) = \left(\frac{R_1}{r_{\lim 1}}\right)^{N_1} + \left(\frac{R_2}{r_{\lim 2}}\right)^{N_2} + \ldots + \left(\frac{R_n}{r_{\lim n}}\right)^{N_n} = \sum_{i=1}^{n} \left(\frac{R_i}{r_{\lim i}}\right)^{N_i} - 1 = 0 \quad (2)$$

N_i in the function is the correlation coefficient describing the dependence between performance limit states, and it determines the shape of multidimensional PLS. The actual value of N_i can be estimated using probabilistic analysis and engineering judgment according to field data or experimental tests. In this framework, limit states can be linear or nonlinear, dependent or independent, random or deterministic. All these options can be formulated as particular cases of the main general one with a suitable choice of *N*.

In the bi-dimensional case of this study, the proposed multidimensional threshold limit state can be expressed by the following Eq. (3). φ_{LS} and ζ_{LS} respectively represent maximum column curvature ductility and maximum longitudinal displacement of bridge bearing. φ_{LSO} and ζ_{LSO} are respectively ductility and displacement thresholds.

$$\frac{\varphi_{LS}}{\varphi_{LSO}} + \left(\frac{\zeta_{LS}}{\zeta_{LSO}}\right)^{N} - 1 = 0 \quad (3)$$

2.3 Performance Limit State Uncertainty

The structural response of spectral ductility-spectral displacement can be represented through "Bell-curve" response, that is the joint probability density function of the response expressed in term of two maximum response variables, which are assumed to be lognormally distributed. Fig. 1 shows a contour plot of the responses in the form of an ellipse (blue line). The red curve represents bi-dimensional performance limit state. Every point on the curve actually follows bi-dimensional lognormal distribution. Probability density funcitons of two points are also plotted in the figure as an example. The performance limit state is not a curve when the uncertainty is considered. Instead, in this study, limit state band is novelly proposed to describe the PLS uncertainty, as shown in Fig. 2. The limit state curve in red is acctual the middle or mean curve of the band.

In order to determin the area of the limit state band quantitatively, confidence interval is firstly proposed in the study to quantitatively describe the lower and upper limit curve for the band. The whole population of limit state random variable *Z* is assumed to be lognormally distributed. The natural logarithm of *Z*, denoted as *X*, is then normally distributed $N(\mu, \sigma^2)$. The objective is to calculate the interval estimation of μ for a given confidence level. Let $X_1, X_2, \ldots X_n$ be the *n* observations that are independent and identically distributed. The random variable *t*-distribution

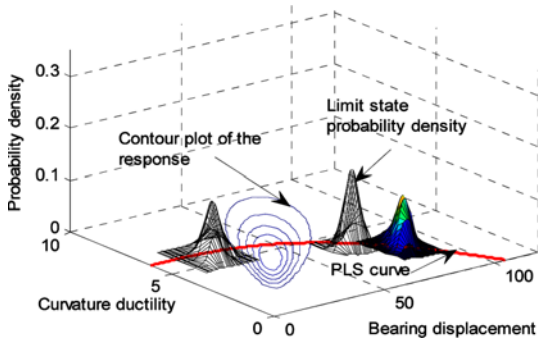

Fig. 1. Uncertainty of PLS

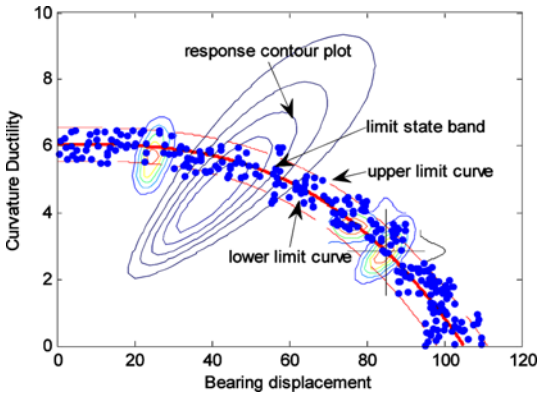

Fig. 2. Bi-dimensional Performance Limit State Band

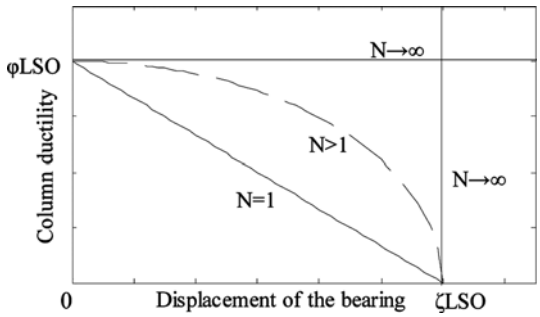

Fig. 3. Bi-dimensional PLS for Different Value of "*N*"

with $n-1$ degrees of freedom, denoted as $T\sim t(n-1)$ is constructed:

$$T = \frac{X-\mu}{S_n^*/\sqrt{n}} \tag{4}$$

Thus for a given confidence level of $1-\alpha$, there exsist a $t_{\alpha/2}(n-1)$ to let the following equation hold.

$$P\{|T| \le t_{\alpha/2}(n-1)\} = 1-\alpha \tag{5}$$

Where $t_{\alpha/2}(n-1)$ is the upper $(\alpha/2)th$ quantile of the $t-$ distribution with $n-1$ degrees of freedom. Then, a $1-\alpha$ confidence interval for μ is constructed.

$$\left[\bar{X}-t_{\alpha/2}(n-1)\frac{S_n^*}{\sqrt{n}}, \bar{X}+t_{\alpha/2}(n-1)\frac{S_n^*}{\sqrt{n}}\right] \tag{6}$$

2.4 Performance Limit State Dependence

The power N in Eq. (3) describes the dependence between different PLSs. The shape the bi-dimensional PLS is determined by the value of N, as shown in Fig. 3. When $N = 1$, the limit state will be a straight line. When $N > 1$, the limit state will be a curve. When $N \to \infty$, the shape of limit state will become two lines parallel to coordinate axes, in which case two PLSs are actually independent. As N increases, the dependence between PLSs weakens and the area of structural failure domain becomes smaller, so the probability of failure decreases. Therefore, the ignorance of dependences between PLSs will result in overestimation of the structural seismic performance, which would be negative for the engineering safety.

3. Case Study

This study presents an investigation of the seismic performance limit state uncertainty and dependence for engineering structures. A reinforcement concrete bridge is used as an example to illustrate the proposed approach. The finite element model is developed in OPENSEES platform. The structural performance limit state threshold is obtained through the Incremental Dynamic Analysis (IDA) method. Through interval estimation, the bi-dimensional limit state band is determined with a confidence level. The correlation coefficient between performance limit states is calculated through nonlinear regression fitting. Consequently, Multidimensional fragility curves with a confidence level can be developed.

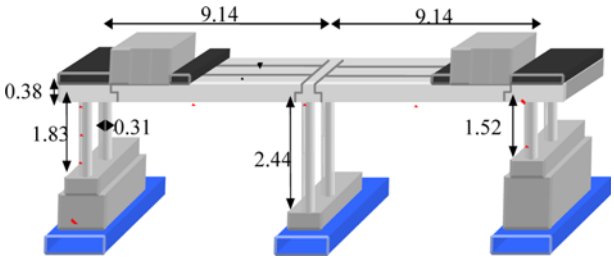

Fig. 4. Case Study Bridge

3.1 Analytical Model for the Case Study Bridge

A three-bent reinforcement concrete bridge in UC Irvine lab (Soyoz 2007) is used as the case study structure (Fig. 4). The bridge deck consisted of three post-tensioned beams. Each of the bents has two columns. To resemble the inertia from the abutments on both ends, additional masses were added. The existence of the post-tension tendons and the pre-stressed strain in the transverse direction made the three individual beams behave as one beam with a large cross section.

The finite element model is developed in OPENSEES. The bridge deck and post-tensioned beams are modeled with beam–column elements. In earthquake excitation, they are expected to be elastic. Nonlinearities of steel bearings and responses of abutment are reflected in the model and they are modeled with nonlinear inelastic springs. The bent columns are represented with fiber models, and bridge foundations with linear rotational and translational springs. The steel 01 element is adopted to model the steel reinforcement. The elastic modulus is 200 GPa. The yield strength is 335 MPa, and the strain-hardening rate is 0.01. The unconstrained concrete is modeled by concrete 02 element. For the element, there are seven physical parameters, which are compressive strength (25.5 Mpa), compressive strength strain (0.002), crushing strength (10 Mpa), crushing strength strain (0.004), the ratio of unloading elastic modulus and the initial elastic modulus (0.1), tensile strength (2.2 Mpa) and tensile softening strength (1100 Mpa).The constrained concrete is also modeled by concrete 02 element, which has the following parameters: compressive strength (28 Mpa), compressive strength strain (0.003), crushing strength (0.018), tensile strength (2.4 Mpa). The fundamental period of the bridge is 0.608s. Nonlinear time history analyses and incremental dynamic analysis are conducted using the platform.

Column and bearing are most likely damaged components for the bridge. Thus, two explicit engineering demand parameters including column curvature ductility and longitudinal displacement of bridge bearing are selected. The column curvature ductility demand (φ) can be express as $\varphi = \theta/\theta_y$. θ is the angle of rotation in column plastic hinge, and θ_y is the rotation angle at the yield point.

Peak Ground Acceleration (PGA) is the maximum ground acceleration of the earthquake excitation. The design basis earthquake ground motion is usually defined in terms of PGA. Thus, PGA has been chosen to characterize seismic ground

motion level in the study (Bojórquez and Iervolino, 2011; Riddell, 2007). The intensity of an earthquake resistance for the structure is 7 degree, with II site classification. The equivalent soil shear wave velocity is 320 m/s. The earthquake design group belongs to the second group. The maximum value of horizontal earthquake influence coefficient is 0.50. According to the structural and site information, the target response spectrum can be calculated and used as input for the earthquake selection. Finally, a suit of 25 earthquake records are determined (Table 1). In the table, *dis* represents epicentral distance. As shown in the Fig. 5, the average spectrum for selected earthquake waves (the red curve) has a good agreement with the target response spectrum (the blue curve). All the earthquake are scaled to be six PGA levels, namely 0.05 g, 0.15 g, 0.35 g, 0.55 g, 0.75 g and 0.95 g for nonlinear time history analysis.

Table 1. Earthquake Record Information

Name (Year)	Station	*Dis*(Km)
Parkfield (1966)	Cholame-Shandon Array #5	9.6
Parkfield (1966)	Cholame-Shandon Array #8	12.9
Managua-Nicaragua-01 (1972)	Managua-ESSO	3.5
Imperial Valley-06 (1979)	Aeropuerto Mexicali	0
Imperial Valley-06	Agrarias	0
Imperial Valley-06	Bonds Corner	0.5
Imperial Valley-06	Brawley Airport	8.5
Imperial Valley-06	Calexico Fire Station	10.4
Imperial Valley-06	Chihuahua	7.3
Imperial Valley-06	Compuertas	13.5
Imperial Valley-06	El Centro Array #10	6.2
Imperial Valley-06	El Centro Array #4	4.9
Imperial Valley-06	El Centro Array #5	1.8
Imperial Valley-06	El Centro Array #6	0
Imperial Valley-06	El Centro Array #7	0.6
Imperial Valley-06	El Centro Array #8	3.9
Imperial Valley-06	El Centro Differential Array	5.1
Imperial Valley-06	Holtville Post Office	5.5
Victoria-Mexico (1980)	Chihuahua	18.5
Victoria-Mexico	Victoria Hospital	6.1
Coalinga-01 (1983)	Pleasant Valley P.P. - yard	7.7
Morgan Hill (1984)	Gilroy Array #2	13.7
Morgan Hill (1984)	Gilroy Array #4	11.5
Morgan Hill (1984)	Halls Valley	3.5
N. Palm Springs (1986)	Palm Springs Airport	10.1

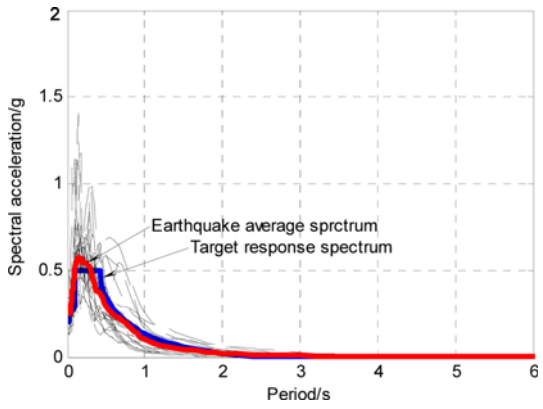

Fig. 5. The Earthquake Average Spectrum

3.2 IDA analysis and Bi-dimensional PLS band

Incremental dynamic analysis is used to obtain structural performance threshold samples, which are assumed to be lognormally distributed. The mean value and standard deviation are evaluated by the maximum likelihood estimation. In the study, 25 seismic records are used for IDA as excitation inputs. The ground motion spectrum acceleration gradually increases from 0 to 0.95 g. Then, column curvature ductility curves and of concrete fiber strain curves that vary with PGA are obtained. Thus, the column concrete strain curves varying with the curvature ductility can be calculated, as shown in Fig. 6. The column strain thresholds for different performance levels are listed in Table 2 (Priestley and Calvi 2003). Considering the mapping relationship between strain and ductility, the mean values of column curvature ductility threshold can be calculated and listed in Table 3. The bearing longitudinal displacement thresholds (mm) can be obtained in the same way. Logarithmic mean value and logarithmic correction standard deviation can also be evaluated. Correlation coefficient N between the two thresholds can be evaluated by nonlinear

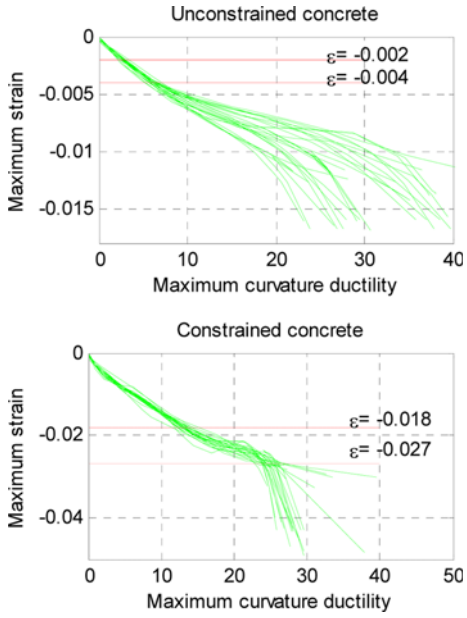

Fig. 6. Maximum Concrete Strain Curves

Table 2. Column Concrete Strain Threshold

Damage state	Concrete strain threshold
Slight	0.002 (unconstrained)
Moderate	0.004 (unconstrained)
Extensive	0.018 (constrained)
Collapse	0.027 (constrained)

Table 3. Performance Limit State Thresholds

Damage	$\mu(\ln\varphi_{LSO})$	$S_n^*(\ln\varphi_{LSO})$	$\mu(\ln\zeta_{LSO})$	$S_n^*(\ln\zeta_{LSO})$
Slight	0.94	0.20	3.42	0.18
Moderate	1.89	0.19	4.67	0.05
Extensive	2.51	0.13	4.95	0.04
Complete	3.24	0.08	5.28	0.03

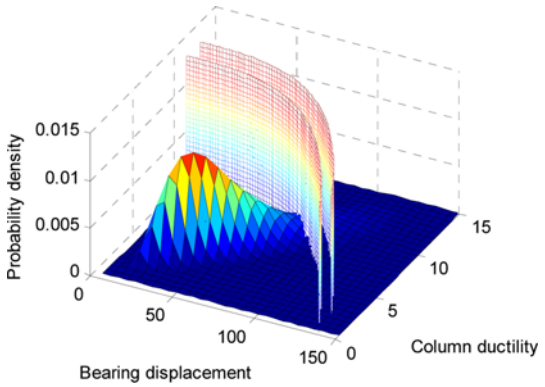

Fig. 7. PLS Upper and Lower Limit Surface

regression analysis, and results are 1.896, 2.231, 2.964 and 4.833 for slight, moderate, extensive damage and collapse performance level, respectively.

For the study, the confidence level is 95%. According to Eq. (6), the lower limits of the 95% confidence interval for curvature ductility are [2.4061 6.2742 11.7535 24.8336]. The upper limits are [2.8428 7.3452 13.1490 26.6609]. The lower limits of the 95% confidence interval for bearing displacement are [29.0287 105.5991 139.9915 194.4573]. The upper limits are [33.8752 110.0407 144.9200 200.1391]. Finally, the performance limit state band for the four damage states can be obtained. Take extensive damage case as an example, the PLS band (both lower and upper limit state curves) is given as Eq. (7). The lower and upper limit state are two surfaces in three-dimensional coordinate system (Fig. 7). The two limit state surfaces are close to each other. The inner suface, which is close to the coordinate zero point, represent the lower limit state. The outer one is the upper limit state surface.

$$\begin{aligned}\text{lower:}&\frac{\varphi}{11.7535}+\left(\frac{\zeta}{139.9915}\right)^{2.964}-1=0\\ \text{upper:}&\frac{\varphi}{13.1490}+\left(\frac{\zeta}{144.92}\right)^{2.964}-1=0\end{aligned}\tag{7}$$

3.3 Probabilistic Seismic Demand Model (PSDM)

Through the nonlinear time history analysis in OPENSEES platform, the maximum curvature ductility and bearing longitudinal displacement are obtained. The logarithmic mean (μ) and logarithmic standard deviation (σ) are evaluated by the maximum likelihood estimation, as shown in Table 4. Then, the correlation coefficient (ρ) of $\ln(\varphi)$ and $\ln(\zeta)$ is calculated. The probability density function of bi-dimensional probabilistic seismic demand model accorded with bivariate lognormal distribution is evaluated.

Table 4. Recorded Maximum Seismic Response

PGA(g)	$\mu(\ln\varphi)$	$\sigma(\ln\varphi)$	$\mu(\ln\zeta)$	$\sigma(\ln\zeta)$	ρ
0.15	0.881	0.321	3.071	0.330	0.765
0.35	1.771	0.401	3.953	0.394	0.914
0.55	2.216	0.310	4.402	0.328	0.929
0.75	2.574	0.356	4.729	0.313	0.784
0.95	2.771	0.403	4.947	0.339	0.794

3.4 Multidimensional Fragility Interval

The multidimensional fragility can be evaluated based on integrating the bi-dimensional PSDM over structural failure domains in Eq. (8).

$$P(\varphi\geq\varphi_{LS}\cup\zeta\geq\zeta_{LS})=\iint_S f(\varphi,\zeta)d\varphi d\zeta\tag{8}$$

The failure domain S is determined by limit state band area. Mathematically, it is defined in the ductility (φ)-displacement (ζ) plan as:

$$\frac{\varphi}{\varphi_{LSO}}+\left(\frac{\zeta}{\zeta_{LSO}}\right)^N-1\geq 0(\varphi\geq 0,\zeta\geq 0)\tag{9}$$

If S is determined by limit state upper curve, the failure domain becomes small. The fragility obtained is actual the confidence lower limit. On the other hand, if the limit state lower curve is selected, the fragility is the confidence upper limit curve. Finally, the fragility intervals with 95% confidence level are generated (Fig. 8). The blue solid curve is the confidence lower limit curve and the black dash one is the lower fragility curve. The probability that the real fragility value falls between these two curves is 95%.

The fragility intervals under the 9 degree earthquake can be read in the Fig. 8. The probability of exceeding slight damage is high. However, the bridge returns to the normal state after simple repairs in this case. The fragility for extensive damage is between 0.55 and 0.67, which are larger than 0.5. Disaster mitigation planning may be made in advance to prevent casualties and economic losses.

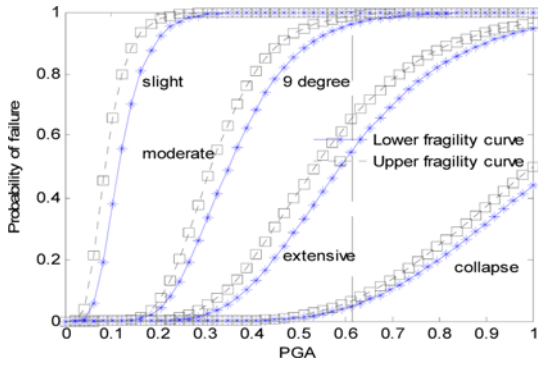

Fig. 8. Fragility Interval with 95% Confidence Level

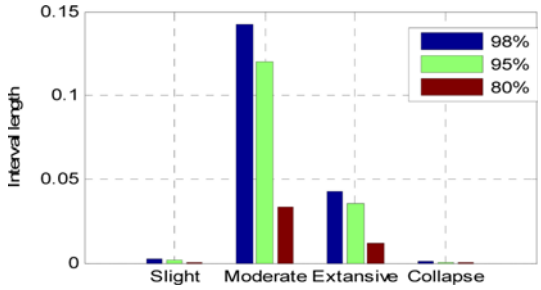

Fig. 9. Fragility Interval Affected by Confidence Level

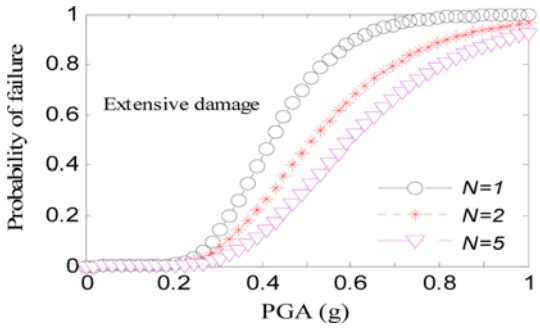

Fig. 10. Sensitivity of the Fragility to Parameter "*N*"

3.5 Sensitivity Analysis of Fragility

The sensitivity of fragility to the confidence level value is investigated. The fragility obtained is actually an interval with a certain confidence level. The fragility interval length is determined by the confidence level. As shown in the Fig. 9, the fragility interval length decreases with the reduction of confidence level. For instance, when the damage state is moderate, the fragility interval length with 98% confidence level is 0.14. When the confidence level is 80%, the interval length becomes 0.03. The length decreases by more than 50 percent. For a real engineering problem, the fragility length is expected to be a narrow one while balancing a relatively high confidence level.

The sensitivity of fragility curves to PLS dependence parameter N is also analyzed. The multi-dimensional fragility curves of the bridge associated with extensive damage states are plotted when $N = 1$, $N = 2$ and $N = 5$, as shown in Fig. 10 (only upper fragility curves are plotted). It can be found that fragility curves fluctuate significantly when N changes. As the value of N increases, the multi-dimensional fragility curves move to the bottom right, so the probability of failure decreases. Fragility become smaller when the dependence between limit states reduce. When the ductility and displacement PLSs are viewed to be unrelated, i.e., $N \to \infty$, unconservative fragility estimation may occur.

4. Conclusions

The study presents a framework to evaluate the multidimensional fragility considering PLS uncertainty and dependence. The limit state band is originally proposed to describe the bi-dimensional PLS function, and the sensitivities of the fragility to the PLS confidence level and dependence are investigated. A reinforcement concrete bridge is used as an example to illustrate the approach. The PSDM accorded with bivariate lognormal distribution is calculated through nonlinear time history analysis. IDA was adopted to analyze structural PLS threshold. Through interval estimation, the bi-dimensional limit state band is determined with a 95% confidence level. Consequently, Multidimensional fragility curves with a confidence level can be generated.

Results show that limit state band can better solve the bi-dimensional PLS uncertainty for fragility analysis. The band area is determined quantitatively through interval estimation and the fragility for the case study bridge with a high confidence level is obtained. The fragility interval is sensitive to the confidence level. With the reduction of confidence level, the interval length decreases and the area between the upper and lower limit curves will become smaller. As the correlation coefficient between PLS thresholds increases, the dependence between PLSs weakens and the probability of failure decreases. Neglecting this statistical dependence can lead to large errors for the fragility estimation.

Acknowledgements

The study was supported by the National Natural Science Foundation of China under Award Number 51278420, Doctorate Foundation under the Grant Number CX201408 and Graduate Starting Seed under the Grant Number Z2016094. The opinions, findings, and conclusions stated herein are those of the authors and do not necessarily reflect those of the sponsors.

References

Bojórquez, E. and Iervolino, I. (2011). "Spectral shape proxies and nonlinear structural response." Soil *Dynamics and Earthquake Engineering*, Vol. 31, No. 7, pp. 996-1008, DOI: 10.1016/j.soildyn. 2011.03.006.

Casciati, F., Cimellaro, G., and Domaneschi, M. (2008). "Seismic reliability of a cable-stayed bridge retrofitted with hysteretic devices." *Computers & Structures*, Vol. 86, No. 17-18, pp. 1769-1781, DOI: 10.1016/j.compstruc.2008.01.012.

Cimellaro, G. P., Reinhorn, A. M., Bruneau, M., and Rutenberg, A. (2006). "Multi-dimensional fragility of structure formulation and evaluation." *Rep. NO. MCEER-06-0002*, University at Buffalo, State University of New York: Multidisciplinary Center for Earthquake Engineering Research., New York.

Cimellaro, G. P. and Reinhorn, A. M. (2010). "Multidimensional performance limit state for hazard fragility functions." *Journal of Engineering Mechanics*, Vol. 137, No. 1, DOI: 10.1061/(ASCE) EM.1943-7889.0000201.

Colangelo, F. (2012). "A simple model to include fuzziness in the seismic fragility curve and relevant effect compared with randomness." *Earthquake Engineering & Structural Dynamics*, Vol. 41, No. 5, pp. 969-986, DOI: 10.1002/eqe.1169.

Colangelo, F. (2013a). "Probabilistic characterisation of an analytical fuzzy-random model for seismic fragility computation." *Structural Safety*, Vol. 40, pp. 68-77, DOI: 10.1016/j.strusafe.2012.09.008.

Karim, K. R. and Yamazaki, F. (2001). "Effects of earthquake ground motions on fragility curves of highway bridge piers based on numerical simulation." *Earthquake Engineering & Structural Dynamics*, Vol. 30,

No. 12, pp. 1839-56, DOI: 10.1002/eqe.97.

Nazri, F. M. and Saruddin, S. N. A. (2015). "Seismic fragility curves for steel and reinforced concrete frames based on near-field and far-field ground motion records." *Arabian Journal for Science And Engineering*, Vol. 40, No. 8, pp. 2301-2307, DOI: 10.1007/s13369-015-1758-y.

Pan, Y., Agrawal, A. K., and Ghosn, M. (2007). "Seismic fragility of continuous steel highway bridges in New York State." *Journal of Bridge Engineering*, Vol. 12, No. 6, pp. 689-699, DOI: 10.1061/(ASCE)1084-0702(2007)12:6(689).

Pang, Y., Wu, X., Shen, G., and Yuan, W. (2014). "Seismic fragility analysis of cable-stayed bridges considering different sources of uncertainties." *Journal of Bridge Engineering*, Vol. 19, No. 4, pp. 1-11, DOI: 10.1061/(ASCE)BE.1943-5592.0000565.

Priestley, M. J. N. and Calvi, G. M. (2003). "Direct displacement based seismic design of concrete bridges." *ACI International Conference on Seismic Bridge Design and Retrofit*, La Jolla.

Riddell, R. (2007). "On ground motion intensity indices." *Earthquake Spectra*, Vol. 23, No. 1, pp. 147-173, DOI: 10.1193/1.2424748.

Soyoz, S. (2007). *Health monitoring of existing structures*, University of California, Irvine.

Tubaldi, E., Barbato, M., and Dall'Asta, A. (2012). "Influence of model parameter uncertainty on seismic transverse response and vulnerability of steel-concrete composite bridges with dual load path." *Journal of Structural Engineering-ASCE*, Vol. 138, No. 3, pp. 363-374, DOI: 10.1061/(ASCE)ST.1943-541X.0000456.